Journal of proteome research

Open Access

pubs.acs.org/jpr

Article

The Proteomic Landscape of Monocytes in Response to Colorectal Cancer Cells

Yiran Wang, Luyao Zhang, Jing Xu, and Jie Ma*

Cite This: https://doi.org/10.1021/acs.jproteome.4c00400

Read Online

ACCESS | Metrics & More | Article Recommendations | Supporting Information

ABSTRACT: Colorectal cancer (CRC) involves a complex interaction between tumor cells and immune cells, notably monocytes, leading to immunosuppression. This study explored these interactions using in vitro coculture systems of THP-1 cells and CRC cell lines, employing quantitative proteomics to analyze protein changes in monocytes. Multiple analytical methods were utilized to delineate the altered proteomic landscape, identify key proteins, and their associated functional pathways for comprehensive data analysis. Differentially expressed proteins (DEPs) were selected and validated by cross-referencing them with publicly available TCGA and GEO data sets to explore their potential clinical significance. Our analysis identified 161 up-regulated and 130 down-regulated DEPs. The enrichment results revealed impairments in adhesion and innate immune functions in monocytes, potentially facilitating cancer progression. The down-regulation of FN1, THSB1, and JUN may contribute to these impairments. Furthermore, the overexpression of ADAMTSL4, PRAM1, GPNMB, and NPC2 on monocytes was associated with unfavorable prognostic outcomes in CRC patients, suggesting potential biomarkers or therapeutic targets. This study illustrated the proteomic landscape of monocytes in response to CRC cells, providing clues for future investigations of the crosstalk between cancer cells and monocytes within the tumor microenvironment.

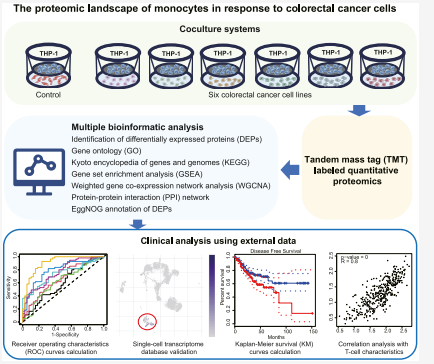

KEYWORDS: *colorectal cancer, monocytes, interactions, quantitative proteome*

INTRODUCTION

Colorectal cancer (CRC) remains a significant global health burden due to its high morbidity and mortality rates.[1] The heterogeneity of CRC, which arises from various genetic, epigenetic, and environmental factors, poses a substantial challenge.[2] Beyond genetic factors, the complexity of CRC also lies in the interactions between cancer cells and the intricate tumor microenvironment (TME).[3] The TME consists of diverse cell types, including fibroblasts, endothelial cells, and immune cells, which interact dynamically with tumor cells, influencing cancer progression and therapeutic responses. Among these, tumor-associated macrophages (TAMs) are particularly notable for their abundance and critical role in immunosuppression. As one of the most abundant components of TME, TAMs play a pivotal role in immunosuppression,[4] implicated in various stages of CRC, from early carcinogenesis to metastatic dissemination. Studies have shown that the majority of TAMs originate from circulating monocytes.[5] Monocytes, which are a key component of the innate immune system, play vital roles in tissue homeostasis and immune defense by responding to pathogens, clearing cellular debris, and modulating inflammation.[6] In-depth research has revealed that monocytes can be recruited to tumors and further polarized toward two types of TAMs. The pro-inflammatory M1 and anti-inflammatory M2 phenotypes exhibit opposing functions, promoting or inhibiting cancer progression.[7] In the context of CRC, the predominance of M2-like TAMs, which support tumor growth, genetic instability, metastasis, and immune evasion, is particularly concerning. The M2 phenotype is predominant in TAMs, promoting cancer genetic instability, supporting metastasis, nurturing cancer stem cells, and taming protective adaptive immunity.[8] Thus, various macrophage-centered approaches to prognostic diagnosis or antitumor therapy are under investigation.[9]

The differentiation of monocytes in tumors results from the response to various signals they receive from the TME, especially the tumor cells. Our previous study[10] has revealed that bestrophin 1 (BEST1) is highly expressed on classical monocytes ($CD14^+CD16^-$) in peripheral blood in head and neck squamous cell carcinoma (HNSCC) patients. This up-regulation by the tumoral VEGF-A cytokine resulted not only in tumor proliferation but also facilitated the monocytes' return to circulation. Similarly, we found this elevation in CRC patients' circulating monocytes, but further investigations were not conducted. Considering the high proportion of infiltrated

Received: May 17, 2024
Revised: July 15, 2024
Accepted: July 30, 2024

macrophages and monocytes in CRC, we focused on the educational effect of CRC tumor cells on monocytes. Previous studies have typically selected a few markers[11] or started from the macrophage stage.[12] In the context of CRC cells, the specific alterations in monocyte behavior induced by these interactions remain underexplored. A comprehensive understanding of these changes is crucial for developing targeted therapies.

Proteins, as the functional executors of cellular processes, serve as critical mediators of the phenotypic manifestations resulting from genomic variability and environmental influences.[13] Therefore, proteomics offers a powerful approach for elucidating molecular mechanisms at the protein level. Proteomics is a high-throughput methodology for comprehensively elucidating molecular mechanisms from a protein perspective. Tandem mass tag (TMT) coupled with liquid chromatography-tandem mass spectrometry (LC-MS/MS) represents a relatively precise and reproducible technology for identifying and quantifying proteins within specimens.

In this study, we used six commonly used CRC cell lines and the human myeloid leukemia mononuclear cell line (THP-1), which is often used when studying human monocytes. In vitro coculture systems were established to investigate changes in monocytes within a purely tumor context. Unlike other studies started from transcriptome level analysis,[14] we directly detected the proteome profile of THP-1 after coculture with CRC cell lines, utilizing TMT-labeled quantitative proteomics. To provide a holistic understanding of the proteomic landscape and the dynamic process of monocyte response to CRC cells, we employed multiple analytical methods. Enrichment analysis of differentially expressed proteins (DEPs), gene set enrichment analysis (GSEA), and weighted gene coexpression network analysis (WGCNA) were employed to explore several evident and specific pathways. Protein−protein interaction (PPI) analysis was for identifying the hub proteins in the processes. Analyses related to external public data using DEPs were also performed to provide insights for establishing diagnosis or prognosis models and finding novel therapeutic targets. Ultimately, we depicted the proteomic landscape of monocytes in response to CRC cells, providing a holistic understanding of this dynamic process.

MATERIALS AND METHODS

Cell Culture and Coculture System

The human CRC cell lines (DLD1, HCT8, HCT116, SW480, SW620, LoVo) and human monocytic leukemia cell line THP-1 were obtained from the Cell Center of the Institute of Basic Medical Sciences, Chinese Academy of Medical Sciences. The normal human colon epithelial cell CCD 841 CoN (CTCC-001−0068) was purchased from Meisen Chinese Tissue Culture Collections (Hangzhou, Zhejiang, China). RPMI 1640 medium (Hyclone, for DLD1, HCT8, and THP-1), Iscove's Modified Dulbecco's Medium (Hyclone, for HCT116), Leibovitz L-15 medium (Gibco, for SW480 and SW620), Ham's F-12K medium (Gibco, for LoVo), and Dulbecco's Modified Eagle's Medium with High Glucose (Hyclone, for CCD 841 CoN) were applied for cell culture, supplemented with 10% fetal bovine serum (Gibco), 100 U penicillin/mL and 100 μg/mL streptomycin (Sigma). All the cell lines were maintained in 5% CO_2 at 37 °C.

According to our previous study,[10] we focus on the noncontact crosstalk between tumor cells and monocytes. Based on this, we used transwell chambers for the coculture system.[15] The CRC cell lines were precultured in 6-well plates at a density of 5×10^5 cells/well. When the cell confluence reached 50%, 0.4 mm transwell insert chambers were placed onto each well, containing THP-1 cells at a density of 5×10^5 cells/well with fresh medium in the chambers. After 3 days of coculture, THP-1 cells were collected. Each group had three repetitions.

Protein Extraction and TMT Labeling

The collected THP-1 cell proteins were extracted using radioimmunoprecipitation assay (RIPA) lysis buffer supplemented with the protease inhibitor PMSF (Solarbio, Beijing). The cells were lysed on ice for 30 min, followed by sonication on ice using a probe sonicator (3 cycles of 10 s with 30-s intervals). The lysates were then centrifuged at 15,000*g* for 20 min at 4 °C to remove cell debris, and the supernatants containing the proteins were collected. Protein concentration was quantified using a BCA assay for further study. Sodium dodecyl sulfate-polyacrylamide gel electrophoresis (SDS-PAGE) was applied for protein quality control. The qualified proteins were then subjected to lysis for reduction and alkylation using a mixture of 1 M DTT, 1 M IAA, UA (8 M urea, 100 mM Tris−HCl, pH 8.0), and 0.5 M TEAB for pretreatment. Subsequently, trypsin was added, and the digestion process was carried out for 12−16 h at 37 °C. Desalination was performed using a C18 Cartridge. The lyophilized peptides were redissolved by 0.1% formic acid and quantified at an absorbance of OD280. Each peptide sample (25−100 μg) was labeled with TMT Label Reagent for 1 h at room temperature and then quenched with hydroxylamine for 15 min, following the instructions provided in the TMT Mass Tagging Kits and Reagents manual (Thermo Fisher Scientific).

LC-MS/MS Detection

The peptides were injected into the reversed-phase trap column C18 (Thermo Scientific, 3 μm, 100 μm × 20 mm), which was connected to the C18 analytical column (Thermo Scientific, 1.9 μm, 150 μm × 120 mm) in buffer A (0.1% formic acid) and separated with a linear gradient of buffer B (80% acetonitrile and 0.1% formic acid) at a flow rate of 600 nL/min, for a total duration of 88 min. The gradient elution was performed at a flow rate of 300 nL/min with the following program: starting with 100% buffer A for 5 min, then increasing buffer B to 9% over the next 31.5 min, followed by a ramp to 18% buffer B. The gradient then increased buffer B from 25 to 30% over 2 min and held at 80% buffer B for the final 5 min. The eluted peptides from the analytical column were directly injected into the mass spectrometer via nano-ESI source. Mass spectrometry was conducted in a data-dependent mode with a full scan resolution of 70,000 and a scan range of m/z 350−1600. Precursor ions were fragmented using high energy collision-induced dissociation with an MS/MS scan resolution of 3500, an isolation window of 2 m/z, and a normalized collision energy of 29. The loop count was set to 20, and dynamic exclusion was applied (charge exclusion: unassigned 1 ≥ 6; peptide match: preferred; exclude isotopes: on; dynamic exclusion: 10 s).

LC-MS/MS analysis was conducted using a Q-Exactive HF-X mass spectrometer (Thermo Scientific) with a runtime of 88 min. The positive ion mode was chosen for the mass spectrometer operation. The scan range was 350−1500 m/z. The automatic gain control (AGC) target was set to 3.0×10^6, with a maximum injection time of 50 ms. Dynamic exclusion

https://doi.org/10.1021/acs.jproteome.4c00400
J. Proteome Res. XXXX, XXX, XXX−XXX

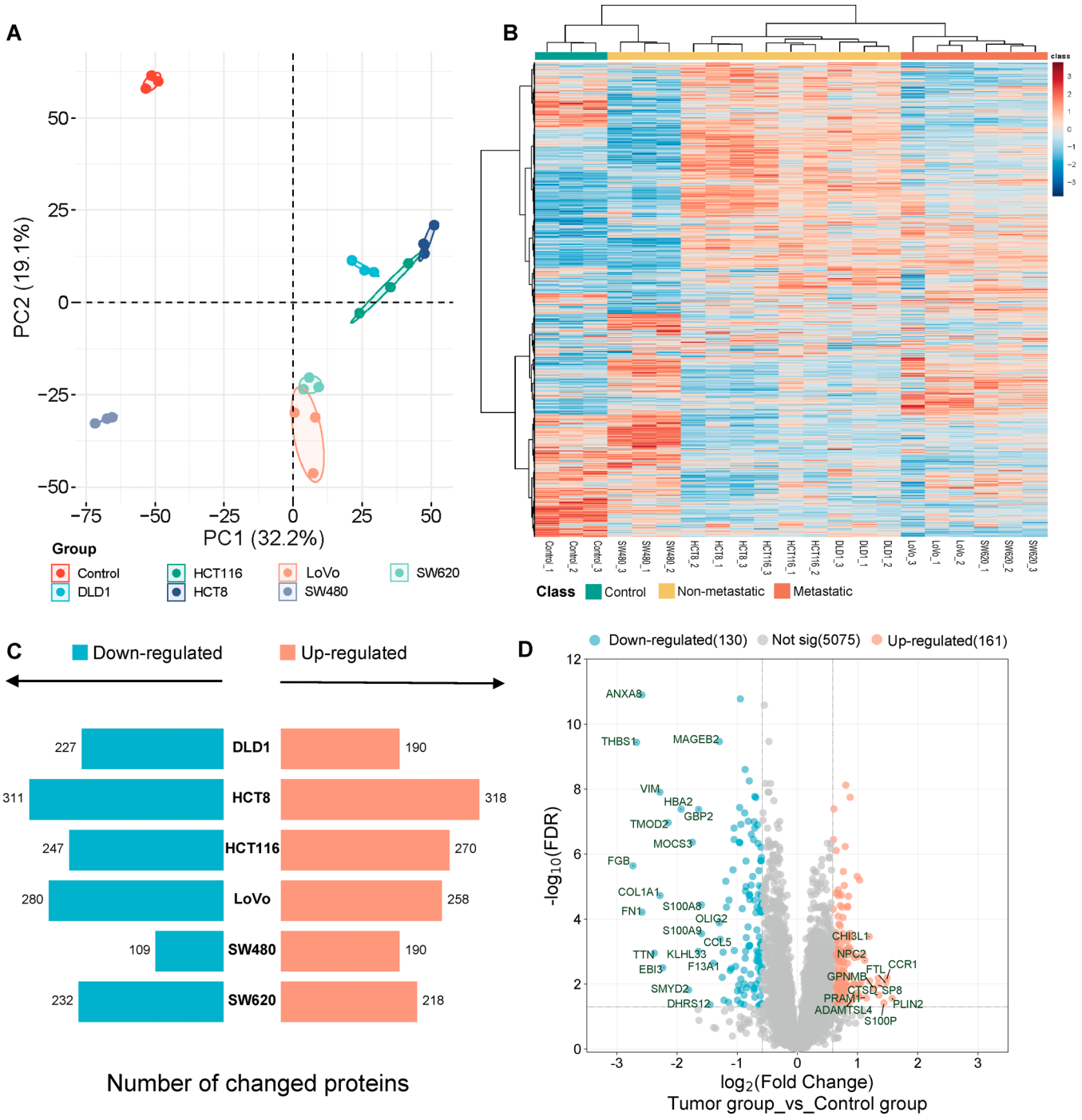

Figure 1. Identification of differentially expressed proteins (DEPs) related to the response of THP-1 to colorectal cancer cell lines. (A) Principal component analysis (PCA) plot of all the samples. (B) Heatmap of all the detected proteins. (C) Butterfly plot of the DEPs in THP-1 cocultured with each CRC cell line, compared to the control. (D) Volcano plot illustrates the DEPs of the tumor group compared with the control, highlighting changed proteins. The threshold for DEPs in this entire figure was set at $|FC| \geq 1.5$ and an adjusted $P < 0.05$.

was set to a duration of 15 s. Survey scans were acquired at a resolution of 120,000 at m/z 200. Peptide data analysis and quantitation were performed using Proteome Discoverer software (Thermo Scientific, version 2.5), with filtration parameters ensuring a peptide FDR $\leq$ 0.01. The analysis used the *Homo sapiens* fasta database downloaded from UniProtKB.

Bioinformatic and Statistical Analysis

Identification of Differentially Expressed Proteins (DEPs) and Enrichment Analysis. DEP identification was conducted using a two-sided unpaired Welch's t test, with the selection criteria of adjusted $P < 0.05$ and |Fold change (FC)| > 1.5. Principal component analysis (PCA) was for data dimension reduction, along with the heatmap and volcano plot to exhibit the whole protein expression landscape. Gene ontology (GO)[16,17] enrichment analysis was applied to assess the functions of DEPs, including biological processes (BP),

https://doi.org/10.1021/acs.jproteome.4c00400
J. Proteome Res. XXXX, XXX, XXX−XXX

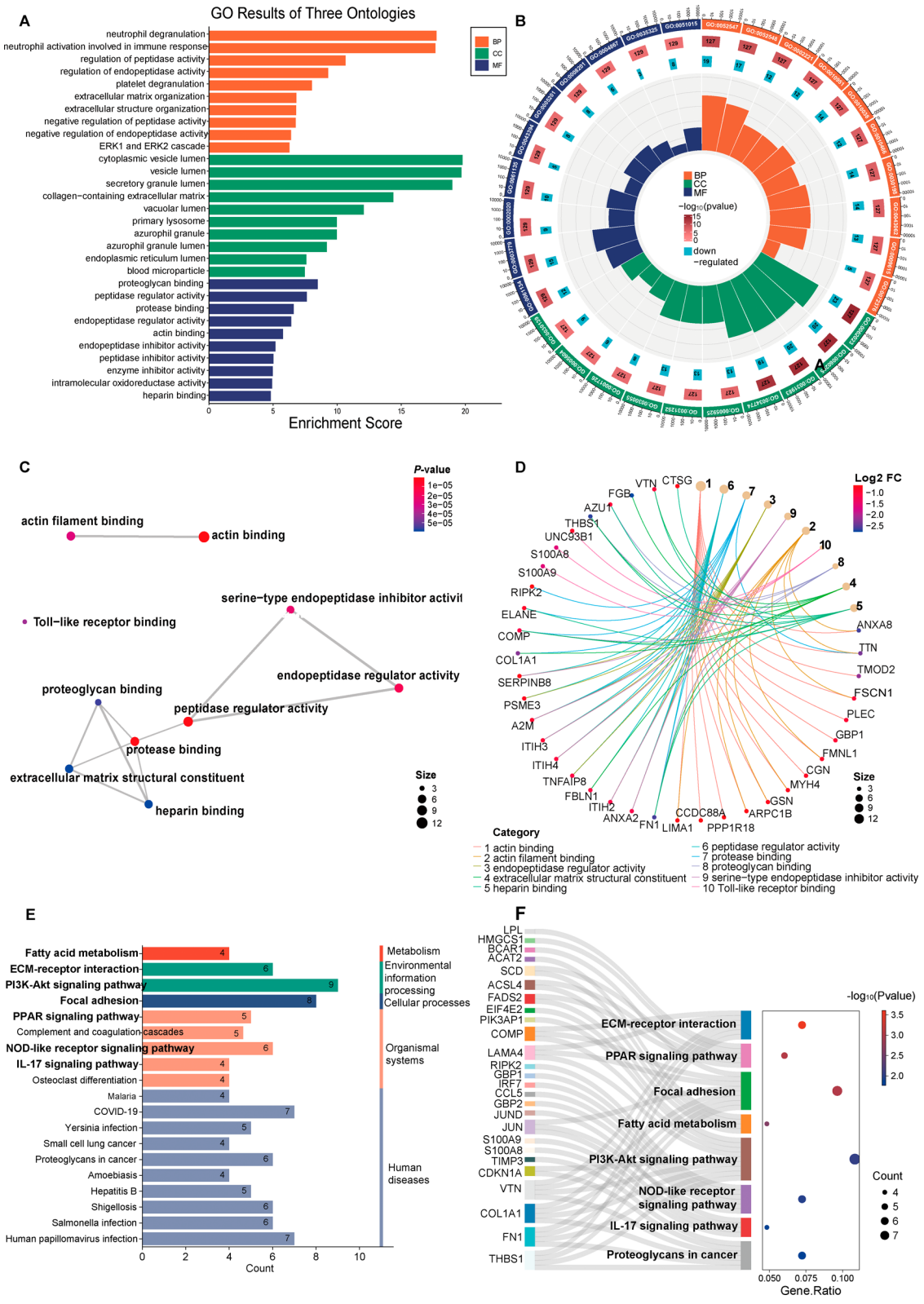

Figure 2. Gene Ontology (GO) and Kyoto Encyclopedia of Genes and Genomes (KEGG) enrichment pathway analysis of DEPs. (A) Barblot of the top 10 enriched pathways in biological process (BP), cellular component (CC), and molecular function (MF) GO categories. (B) Visualization of the down-regulated DEPs enriched in GO pathways. The detailed information is shown in Table 1. (C) Emapplot for depicting the enrichment map for the top 10 enriched pathways of the down-regulated DEPs in the MF category. The lines in the plot represent gene overlap relationships among enriched GO terms. (D) Cnetplot exhibits the relationships between the top 10 enriched down-regulated pathways in the MF category and the involved DEPs. (E) Classified KEGG pathways of the down-regulated DEPs. (F) Sankey and dot plot visualized the selected KEGG pathways and the involved DEPs.

https://doi.org/10.1021/acs.jproteome.4c00400
J. Proteome Res. XXXX, XXX, XXX−XXX

Table 1. Detailed Gene Ontology (GO) Analysis Results of Down-Regulated Pathways across Three Ontologies[a,b]

GO term		description	GO term		description
GO:0052547	BP	regulation of peptidase activity	GO:0031252	CC	cell leading edge
GO:0052548	BP	regulation of endopeptidase activity	GO:0030055	CC	**cell-substrate junction**
GO:0002221	BP	**pattern recognition receptor signaling pathway**	GO:0001726	CC	ruffle
GO:0010951	BP	negative regulation of endopeptidase activity	GO:0005604	CC	basement membrane
GO:0010038	BP	response to metal ion	GO:0030139	CC	endocytic vesicle
GO:0010466	BP	negative regulation of peptidase activity	GO:0061134	MF	peptidase regulator activity
GO:0030198	BP	**extracellular matrix organization**	GO:0003779	MF	actin binding
GO:0043062	BP	extracellular structure organization	GO:0002020	MF	protease binding
GO:0009615	BP	**response to virus**	GO:0061135	MF	endopeptidase regulator activity
GO:0072376	BP	protein activation cascade	GO:0043394	MF	proteoglycan binding
GO:0062023	CC	**collagen-containing extracellular matrix**	GO:0005201	MF	**extracellular matrix structural constituent**
GO:0060205	CC	cytoplasmic vesicle lumen	GO:0008201	MF	heparin binding
GO:0031983	CC	vesicle lumen	GO:0004867	MF	serine-type endopeptidase inhibitor activity
GO:0034774	CC	secretory granule lumen	GO:0035325	MF	**Toll-like receptor binding**
GO:0005925	CC	**focal adhesion**	GO:0051015	MF	actin filament binding

[a]BP: Biological Process; CC: Cellular Component; MF: Molecular Function. [b]Bold texts indicate the pathways that are consistent with the KEGG results.

cellular components (CC), and molecular function (MF) ontologies. The Kyoto encyclopedia of genes and genomes (KEGG) pathway[18] was also for enrichment analysis of DEPs. The R package clusterProfiler4[19] and pathview[20] were performed for GO and KEGG calculation and visualization.

Gene Set Enrichment Analysis (GSEA). GSEA was performed to assess the significance of an a priori-defined set of genes in two biological states.[21] The priori-defined sets were those pathways of GO and KEGG. We considered pathways with |NES| > 1.5 and $P < 0.05$ as statistically significant. The R package clusterProfiler was still for enrichment analysis, while the aPEAR[22] was utilized for the GSEA pathways clustering.

Weighted Gene Coexpression Network Analysis (WGCNA). WGCNA, implemented using the WGCNA R software package,[23] was applied to all proteins, not just the DEPs, to construct a coexpression network and identify modules. We computed the module-trait correlations between the modules and the cancer traits. The proteins included in the most relevant module were chosen for further KEGG enrichment analysis using KOBAS (http://bioinfo.org/kobas/).[24]

Protein−Protein Interaction (PPI) Network. The STRING database (version 11.5) (www.string-db.org)[25] was used to construct the PPI network to elucidate the interactions between target proteins. Proteins with connections were subsequently assessed for their degree[26] and visualized by importing them into Cytoscape software.[27]

EggNOG Annotation of DEPs. EggNOG (evolutionary genealogy of genes: Nonsupervised Orthologous Groups) database 5.0 (http://eggnogdb.embl.de/) is an extension of the COG (Cluster of Orthologous Groups of proteins).[28] This method classifies protein sequences into different orthologous clusters based on their similarity, enabling the annotation of the function of unknown proteins by comparing them with known proteins in the same cluster.

Clinical Analysis Using External Data. GEPIA2021 (http://gepia2021.cancer-pku.cn/) is an enhanced web server that integrates multiple deconvolution-based analyses into the GEPIA platform, incorporating data from the TCGA and GTEx projects.[29] We applied it to investigate gene changes during the monocyte polarization process in CRC tissue. The GSE47756 data set[30] was an expression profiling by array, which contained data of peripheral blood monocytes from 93 individuals (38 healthy volunteers, 27 patients with non-metastatic colorectal cancer, and 28 patients with metastatic colorectal cancer). In this data set, we analyzed the DEPs selected from our results to discover some clues that may be connected with clinical status. Receiver operating characteristic (ROC) curves were generated using the data in this data set using easyROC (http://www.biosoft.hacettepe.edu.tr/easyROC/).[31]

To explore more potential clinical meanings of the target proteins, we applied the scRNA analysis database TISCH2 (http://tisch.comp-genomics.org/home/)[32] to investigate whether the significantly elevated proteins exhibited specific or high expression on monocytes/macrophages within colorectal cancer tissues. TISCH2 is a comprehensive database for single-cell RNA sequencing data, which provides detailed cell type annotation and enables exploration of gene expression at the single-cell level across various cancer types. Following this analysis, we examined the association between these proteins and clinical outcomes using CRC data sets (TCGA-COAD and TCGA-READ). The Kaplan−Meier (KM) curves were generated using the GEPIA2 web tool (http://gepia2.cancer-pku.cn/).[33] GEPIA2 is also an updated and enhanced version of GEPIA, which offers fast and customizable functionalities for gene expression profiling and interactive analysis based on TCGA and GTEx data.

RESULTS

Identification of DEPs in THP-1 Cocultured with CRC Cells

The protein expression profile was investigated using TMT-based proteomics to understand the mechanisms underlying THP-1's response to CRC cells. A total of 53269 peptides were identified (Table S1). The results related to quality control can be found in Figure S1. We detected 7007 unique proteins (Table S2), with 5366 of them observed in all samples. The PCA plot (Figure 1A) and heatmap (Figure 1B) showed minimal differences within the groups but significant differences between them, suggesting that THP-1's protein expression did change under the influence of CRC cells. It was evident that the metastatic CRC cells (SW620 and LoVo) had a different impact on monocytes compared to non-

https://doi.org/10.1021/acs.jproteome.4c00400
J. Proteome Res. XXXX, XXX, XXX−XXX

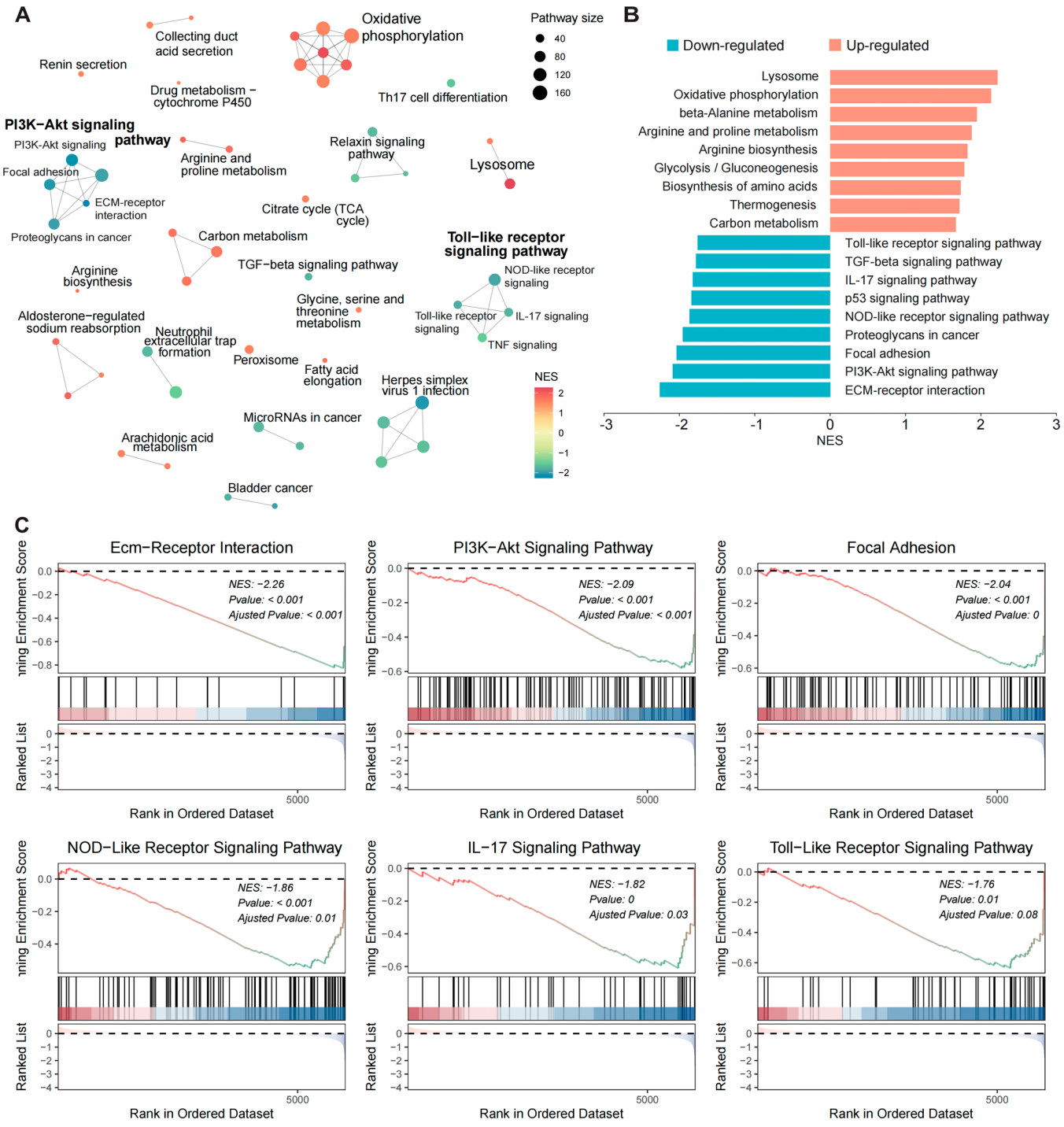

Figure 3. Gene set enrichment analysis (GSEA) of KEGG pathways. (A) Visualization displays pathway enrichment networks, representing similarities between pathway gene sets as interconnected clusters. (B) Bidirectional barplot of the top 9 (excluding pathways related to disease) up-regulated and down-regulated pathways by GSEA. (C) The six significantly enriched ($P \leq 0.01$) KEGG pathways identified by GSEA corresponded to the results of DEP enrichment analysis.

metastatic CRC cells (DLD1, HCT-8, HCT116, SW480). The degree of protein changes correlated with the malignancy of the tumor cells. When compared individually to the control, different CRC cell lines exhibited varying alterations in the regulation of THP-1 (Figure 1C and Table S3). To explore the commonality of these changes, we first defined THP-1 coculture with all the CRC cell lines as the tumor group and compared it with the control group (coculture with CCD841CoN). This analysis identified a total of 161 up-regulated and 130 down-regulated proteins (Figure 1D and Table S3), which were defined as differentially expressed proteins (DEPs).

Different Functional Enrichment Analyses Yielded Consistent Results

We then conducted GO and KEGG functional enrichment analyses using the identified DEPs. The top 10 GO term annotations in three ontologies are presented in Figure 2A. We further enriched both up-regulated and down-regulated DEPs

https://doi.org/10.1021/acs.jproteome.4c00400
J. Proteome Res. XXXX, XXX, XXX−XXX

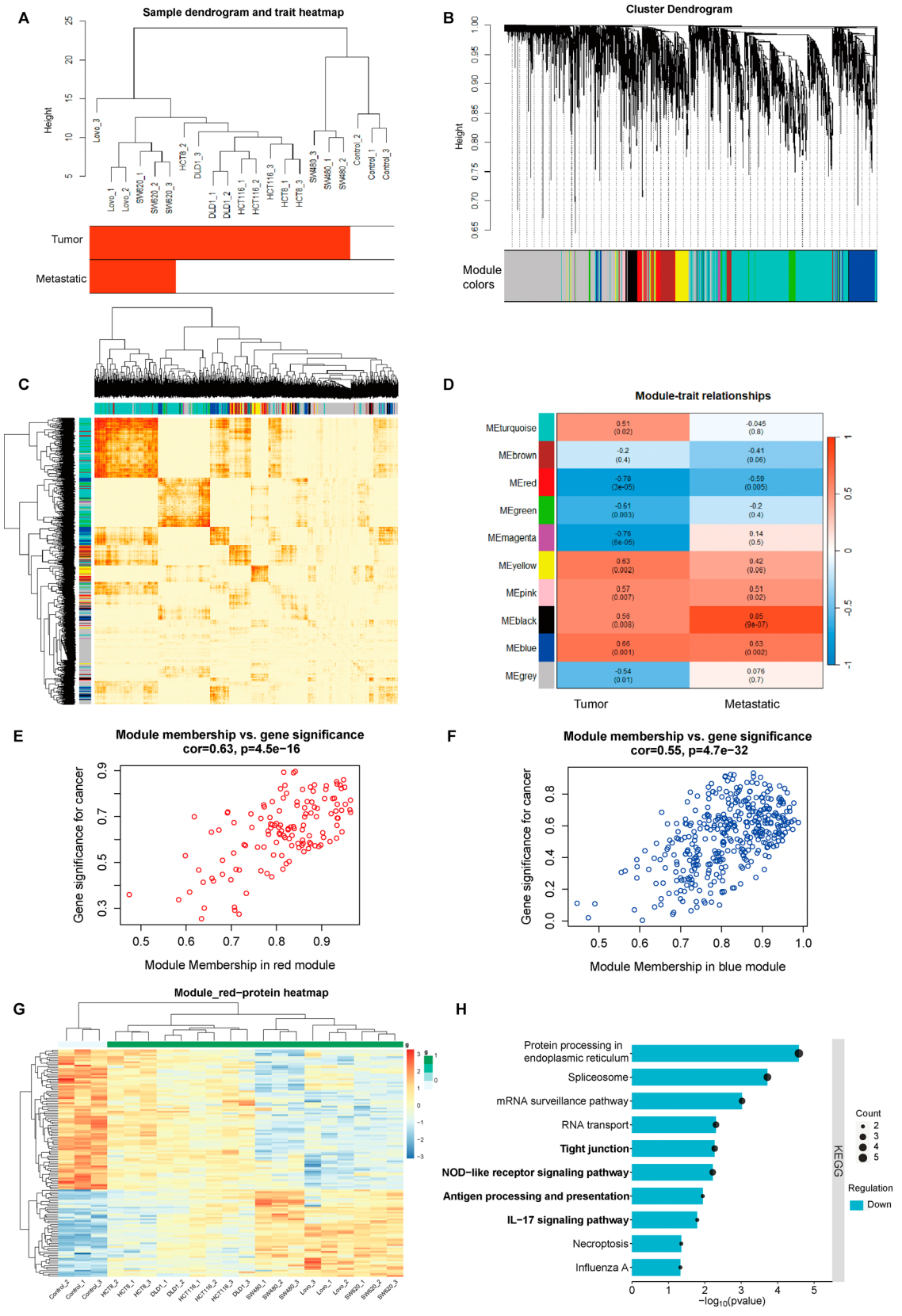

Figure 4. Identification of protein modules associated with the response of monocytes to CRC using weighted gene coexpression network analysis (WGCNA). (A) Hierarchical clustering dendrogram of the samples. (B) Clustering dendrogram of all detected proteins. (C) Network heatmap plot depicting the topological overlap matrix (TOM) among all the detected proteins. (D) Module-trait relationships illustrating the associations between the tumor and metastatic signatures and the proteins in each module. (E, F) Scatter plots showing the correlation between the significance of proteins for the tumor group and proteins in the red and blue modules. (G) Heatmap of the proteins in the red module. (H) KEGG pathways associated with the down-regulated DEPs in the red module.

https://doi.org/10.1021/acs.jproteome.4c00400
J. Proteome Res. XXXX, XXX, XXX−XXX

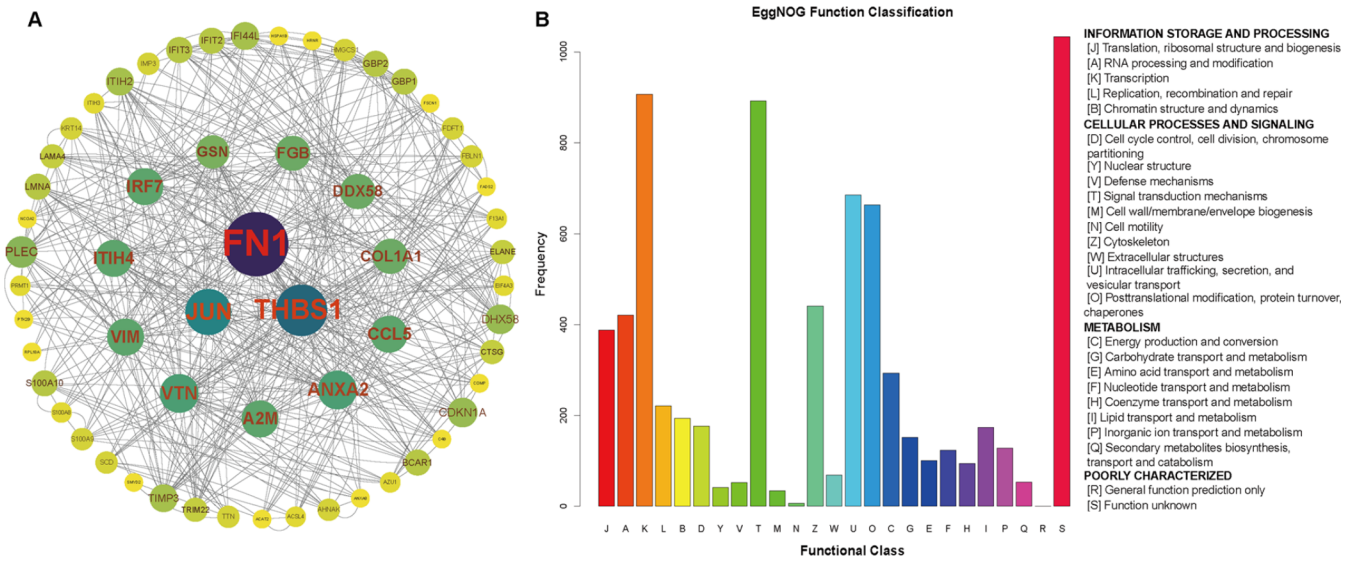

Figure 5. Other protein analyses. (A) Protein−protein interaction (PPI) network of the down-regulated DEPs. (B) Statistical results of eggNOG annotation.

separately. Given that the stimulated pathways predominantly pertained to metabolic processes (Table S4), the suppressed pathways were associated with various functional aspects. We mainly put an eye on the reduced proteins and their functions. Figure 2B and Table 1 display the GO enrichment results, revealing the abilities of THP-1 that were impaired by CRC cells.

When further analyzing the MF category (Figure 2C,D), besides the ability to bind various substances, we noticed a term related to innate immune response (Toll-like receptor binding). Consistent with the bolded results of GO in Table 1, the KEGG results (Figure 2E,F) revealed significant enrichment of adhesion-related pathways (ECM-receptor interaction and focal adhesion) and innate-immune-related pathways (NOD-like receptor signaling pathway and IL-17 signaling pathway) among the down-regulated DEPs.

To further validate the KEGG results, we employed the GSEA method. The cluster of significant pathways (Figure 3A) also emphasized these functions (PI3K-Akt signaling pathway cluster and Toll-like receptor signaling pathway cluster). They were also the most noticeable suppressed signaling in further analysis (Figure 3B,C). Thus, even considering all the proteins detected, the PI3K-Akt signaling pathway, Toll-like/NOD-like receptor signaling pathway, and ECM-receptor interaction pathway were also remarkably down-regulated. Detailed results can be found in Table S5.

Identification of Protein Modules Associated with the Response of Monocytes to CRC and Functional Enrichment Analysis

We proceeded to conduct WGCNA to delve deeper into the analysis. This distinct analytical approach also demonstrated a strong clustering among the samples (Figure 4A). WGCNA divided all the proteins into 10 modules (Figure 4B,C). By calculating the correlation between the modules and the tumor group (Figure 4D), the red module (Figure 4E,F) indicated the most relevant relationship. After extracting the proteins in the red module (Figure 4G and Table S6), the decreased proteins (FC < 0, P < 0.05) were enriched (Figure 4H). The pathways of tight junction (similar to focal adhesion), NOD-like receptor signaling, and IL-17 signal overlapped with the significant results of GSEA. The pathway of antigen processing and presentation is also one of the innate immune functions in monocytes.

Selection of Node DEPs via the PPI Network

According to the PPI results (Figure 5A), FN1, THBS1, and JUN were the top three proteins interacting with other down-regulated DEPs, indicating that they may function as hub proteins in the suppressed pathways. Among the node proteins (degree >25, 14 in the protein circle), FN1, THBS1, VTN, and COL1A1 could be annotated to the KEGG pathways of ECM-receptor interaction, Focal adhesion, PI3K-Akt signaling, and Proteoglycans in cancer. Meanwhile, CCL5, IRF7, and DDX58 were involved in some inflammatory-related pathways (NOD-like receptor signaling, Toll-like receptor signaling, RIG-I-like receptor signaling, and Cytosolic DNA-sensing, as shown in Supporting Table 4).

Statistical Results of eggNOG Annotation

EggNOG provided a different way to classify those changed proteins (Figure 5B). The alterations mainly took place on "Transcription" (count of 907), "signal transduction mechanisms" (892), "intracellular trafficking, secretion, and vesicular transport" (685), and "posttranslational modification, protein turnover, chaperones" (663). As for metabolism functions, proteins aggregated on the 'Energy production and conversion' mostly.

Differences between Metastatic and Nonmetastatic CRC Cell Line Effects on THP-1

Among the CRC cell lines we studied, SW620 and LoVo are metastatic. We further defined THP-1 coculture with them as the metastatic group and analyzed their characteristic using the methods mentioned before. In comparison with the non-metastatic group (THP-1 coculture with DLD-1, HCT-8, HCT116, and SW480 cells), we identified 70 up-regulated and 42 down-regulated DEPs (ME-DEPs: DEPs of the metastatic group, Figure 6A). Figure 6B,C displays the GO results of the ME-DEPs. The KEGG results (Figure 6D) suggested that the influence of metastatic CRC cells on monocytes mainly involved the activation of lysosome and Glycosaminoglycan degradation pathways while suppressing the Phospholipase D

https://doi.org/10.1021/acs.jproteome.4c00400
J. Proteome Res. XXXX, XXX, XXX−XXX

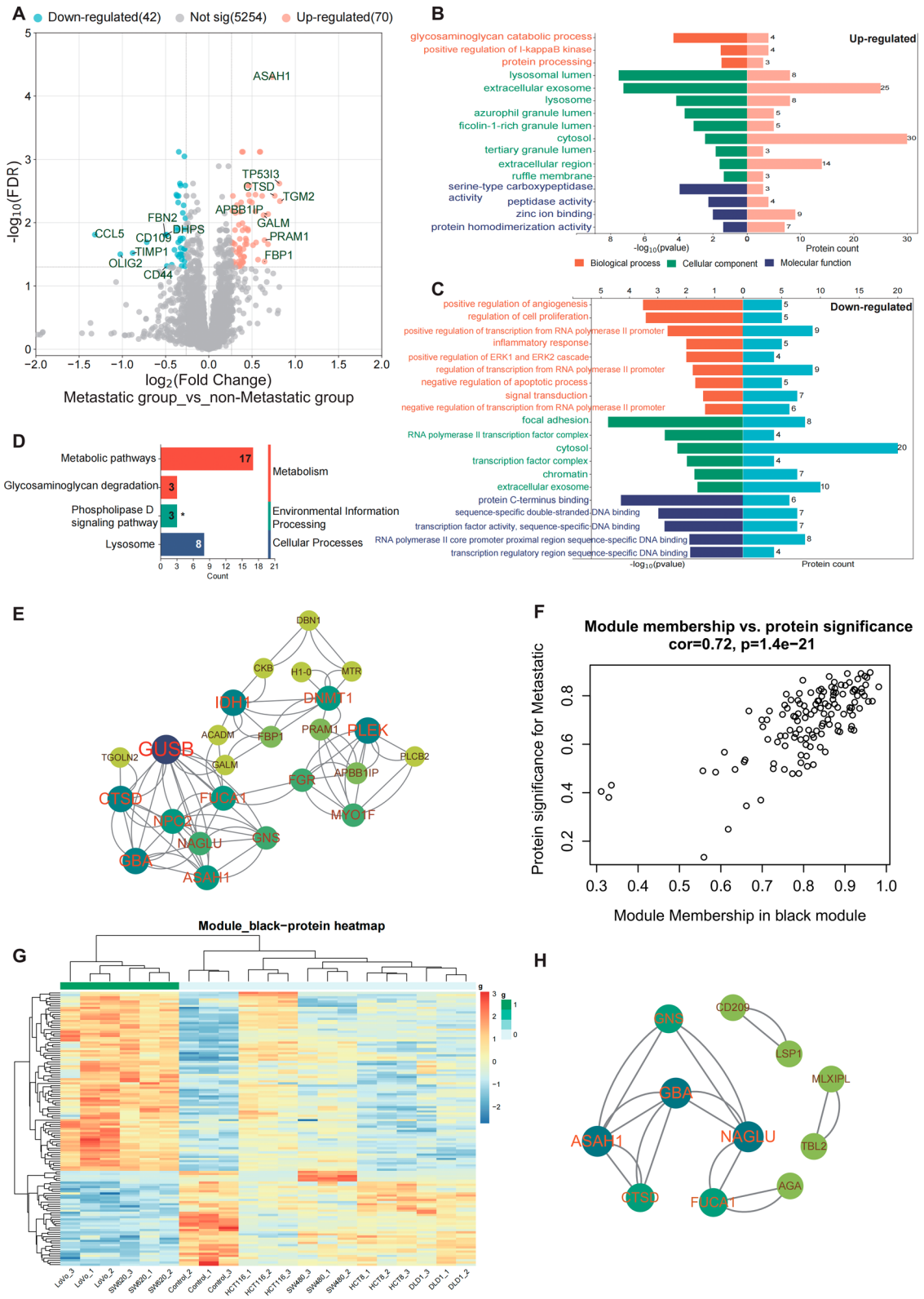

Figure 6. Analysis of the metastatic group compared to the nonmetastatic group. (A) Volcano plot illustrates the DEPs of the metastatic group compared with the nonmetastatic group (ME-DEPs). The threshold of DEPs was $|FC| \geq 1.2$ and the $P < 0.05$. (B, C) Significantly up-regulated and down-regulated GO pathways ($P < 0.05$) were enriched by ME-DEPs. (D) KEGG pathways with statistical significance. *The Phospholipase signaling pathway was down-regulated while the others were up-regulated. (E) PPI network of the ME-DEPs. (F) Scatter plot based on WGCNA depicting the correlation between the protein significance for the metastatic group and proteins in the black modules. (G) Heatmap of the proteins in the black module by WGCNA. (H) PPI network of the up-regulated proteins in the black module.

signaling pathway. The PPI network (Figure 6E) shows some hub proteins. In the WGCNA part, we observed that the black modules were mostly related to the metastatic status with a correlation coefficient of 0.72 (Figure 6F). It is evident that

https://doi.org/10.1021/acs.jproteome.4c00400
J. Proteome Res. XXXX, XXX, XXX−XXX

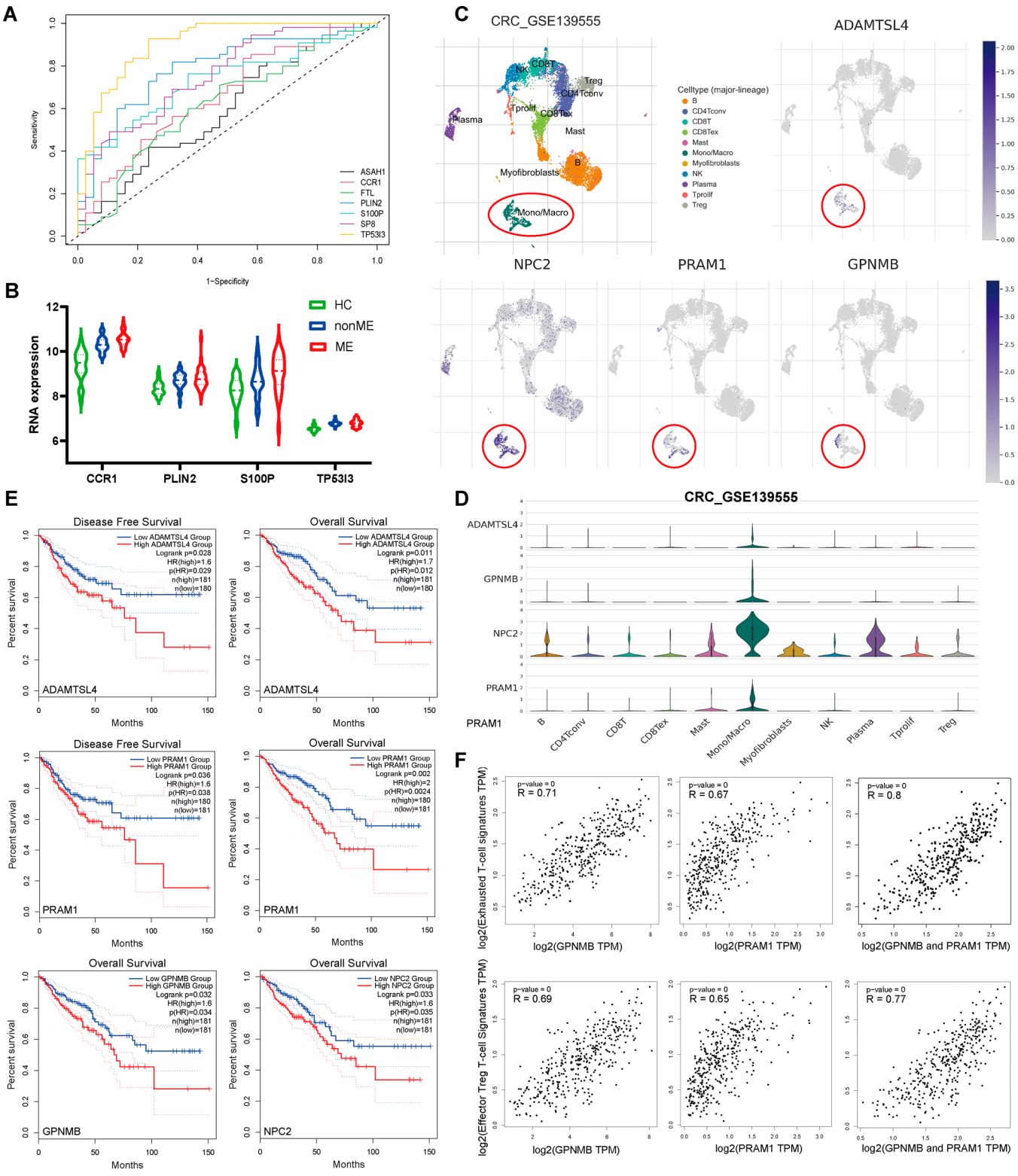

Figure 7. Clinical analysis using external data. (A) Receiver operating characteristic (ROC) curves of 7 candidate biomarkers (proteins markedly elevated in our results) in the GSE47756 data set. (B) The expression of 4 candidate biomarkers (increased with the malignancy of the disease) in healthy control (HC), primary CRC patients (nonME), and metastatic CRC patients (ME) in the GSE47756. (C, D) The visualization of 4 genes (ADAMTSL4, GPNMB, NPC2, and PRAM1) that were specific or highly expressed on monocytes/macrophages within colorectal cancer tissues in the GSE139555 data set. (E) Kaplan−Meier (KM) curves analyzing the association between the expression levels of the specific four genes (ADAMTSL4, GPNMB, NPC2, and PRAM1) and clinical outcomes (disease-free survival and overall survival) of CRC patients in TCGA data sets. (F) Analysis of correlations between genes and signatures of immunosuppressed T cells.

among the proteins in the black module, the majority were up-regulated (Figure 6G). We further analyzed the PPI among the up-regulated proteins in the black modules (Figure 6H). By integrating the PPI results from Figure 6E,6H, it becomes

https://doi.org/10.1021/acs.jproteome.4c00400
J. Proteome Res. XXXX, XXX, XXX−XXX

apparent that GUSB, CTSD, ASAH1, FUCA1, NAGLU, and GNS may play pivotal roles in the influence of metastatic CRC cells on monocytes. In addition, we compared ME-DEPs and DEPs of tumor cells versus controls (Figure S2), revealing that metastatic CRC more significantly impaired the ECM-receptor interaction ability in THP-1 cells, although different proteins were involved. All the detailed results in this section are in Table S7.

Possible Clinical Meanings of the Selected DEPs

For diagnostic purposes, upregulated markers are often more reliable and easier to detect in clinical settings. Hence, we conducted an exploration using GEPIA2021, incorporating the node proteins obtained from the PPI analysis of upregulated differentially expressed proteins in two differential analyses (comparing metastatic CRC cell lines vs nonmetastatic CRC cell lines and tumor group vs control group). We observed that except for some genes lacking data in TCGA, the corresponding genes for other proteins were highly expressed in M2-like macrophages (Figure S3). Based on this, we infer that CRC cells predominantly induce monocytes to differentiate toward the M2 phenotype in the TME.

Next, we proceeded to validate the upregulated DEPs (the top 10 from both analyses) by integrating them with transcriptome data (GSE47756) from peripheral blood monocytes of colorectal cancer patients. In this analysis, TP53I3 emerged as a potential biomarker with diagnostic efficacy (Figure 7A). Simultaneously, while CCR1, PLIN2, and S100P may not distinguish between primary and metastatic tumor patients, they do exhibit an association with disease malignancy, with their expression levels increasing as the disease progresses (Figure 7B).

Take it to the next level, by integrating scRNA data with bulk survival data, we discerned specific expression of ADAMTSL4 and PRAM1 on monocytes within colorectal tumor tissues even in different data sets (Figures 7C,D and S4). Notably, the high expression of these two genes in colorectal tumor tissues is associated with poor overall survival (OS) and disease-free survival (DFS) (Figure 7E). In addition, the specific expression of GPNMB and the highest expression of NPC2 on monocytes/macrophages are both correlated with short DFS (Figure 7E).

To dig deeper, we analyzed the correlation between these four genes and the signature genes of different T cell categories to preliminarily investigate the potential immunosuppressive function of monocytes/macrophages expressing these genes. Strikingly, the coexpression of GPNMB and PRAM1 was highly correlated with the T-cell exhaustion and Treg T-cell signatures (Figure 7F), hinting the coexistence of $GPNMB^{+}PRAM1^{+}$TAMs potentially signify an immunosuppressive and exhausted $CD8^{+}$ tumor-infiltrating lymphocyte population.

DISCUSSION

CRC has a high prevalence and mortality globally and limited benefits from immune checkpoint inhibitors (ICIs).[1] CRC is referred to as a type of "cold tumor", with a low abundance of T cells, presenting significant challenges in immunotherapy.[34] The generally insufficient response rate is not only attributed to the high heterogeneity of CRC but also the complexity of the TME. The TME is a multifaceted and dynamic ecosystem with a pivotal influence on tumor growth, advancement, and treatment response. Apart from the cancerous cells, other cells play essential roles by interacting with them, including stromal fibroblasts, endothelial cells, and immune cells. These cells possess distinctive immunological abilities that can either inhibit or enhance tumor development. The major component of immune cells, TAMs, has driven plenty of studies.[5,35] The plasticity of TAMs bestows them a dual role in tumor development.[36] Based on the fact that TAMs primarily originate from circulating monocytes, we kept an eye on the regulation of monocytes by tumor cells. Our previous study[10] revealed that head and neck squamous cell carcinoma (HNSC) cells altered the molecular expression of monocytes, which transformed into a phenotype conducive to tumor growth. Simultaneously, it induced monocytes to re-enter the blood circulation, facilitating the utilization of these altered molecules as diagnostic markers for HNSC patients. Considering the relatively high abundance of infiltrated monocytes in CRC,[37] we further investigated how CRC cells influence monocytes. In this study, after coculturing the monocyte cell line THP-1 with six common CRC cell lines for 3 days, we examined the proteome of THP-1 and analyzed it with various methods. This enabled us to gain insight into the impact of extracellular factors tumor-secreted on monocytes. Our comprehensive analysis may offer valuable clues for future experimental studies and the potential clinical applications of monocytes.

By employing three distinct techniques (enrichment analysis of DEPs, GSEA, and WGCNA) to reveal the functional alterations, it was readily apparent that monocytes had experienced impairments in two prominent aspects: (i) ECM receptor interaction and focal adherent; (ii) NOD-like receptor signaling and Toll-like receptor signaling.

The extracellular matrix (ECM) is a dynamic network that regulates cell behavior and tissue homeostasis.[38] When analyzing the whole CRC tissue data, the RNA-seq would exhibit that the elevated signal of interaction between ECM and cellular receptors is beneficial for cancer progression and metastasis.[39] But the situation differs if concerns the monocytes separately. Under the mediation of integrin, interaction of monocytes with ECM leading to the regulation of gene expression, involved in inflammation and immune responses.[40] This pathway and another reduced function "focal adherent" also can synergize to enable the circulating monocytes to locate and adhere. Adherent monocytes and infiltrated macrophages can release cytokines and propagate inflammatory responses.[41] Hence, our results indicated that CRC cells impair the ECM receptor interaction and the focal adherence functions of monocytes, fundamentally compromising the monocytes' immune and inflammatory capabilities.

The NOD-like receptor (NLR) signaling pathway is fundamental for monocytes and has been widely investigated. NLRs are a group of evolutionarily conserved pattern recognition receptors (PRRs) critical for microbial recognition and host defense. The weakened Toll-like receptor (TLR) pathway is also involved in PRRs.[42] They are highly conserved cytosolic receptors that perform critical functions in surveying the intracellular environment for the presence of infection, noxious substances, and metabolic perturbations. Coillard et al.[43] disclosed that the detection of pathogens can influence the initial step in monocyte differentiation, where TLR signaling generally promotes macrophage development, while NOD receptor signaling triggers dendritic cell differentiation. This attenuated differentiation and adhesion capacity are coordinated, both contributing to the reduced infiltration of monocytes. Furthermore, the role of intratumoral microbiota

https://doi.org/10.1021/acs.jproteome.4c00400
J. Proteome Res. XXXX, XXX, XXX−XXX

in the development and progression of CRC has been increasingly recognized.[44] The compromised innate immune capabilities of monocytes may also act as accomplices in bacterial infiltration and intratumoral bacterial-mediated tumor progression.

When focusing on the specific down-regulated proteins, the PPI analysis of DEPs pointed to three hub proteins for us: fibronectin (FN1), thrombospondin-1 (THBS1), and transcription factor Jun (JUN). FN1 is a versatile glycoprotein in the ECM, involving cellular growth, differentiation, adhesion, and migration through integrin-mediated signaling.[45] Physically, FN1 is majorly produced by fibroblasts to assist in tissue development and homeostasis and is crucial in interacting with other cells.[46] In the context of cancer, FN1, specially produced by cancer-associated fibroblasts (CAF) has been identified an indispensable role for tumor onset and progression.[47] In our results, this "risk factor" was down-regulated. Does that indicates an antitumor effect? Since the pro-tumoral FN1 is not predominantly produced by monocytes, the down-regulation of FN1 in monocytes should primarily impact the monocytes themselves. Madsen et al.[48] identified a type of collagen-degrading TAMs, which originated from circulating monocytes and belong to M2-like TAMs. They remodel a promote-tumor microenvironment by degrading collagen in a mannose receptor-dependent manner. These TAMs were characterized as a low expression of collagen genes, including fibril-forming collagens, basement membrane collagens, fibril-associated collagens with interrupted triple helices, proteoglycans, and other ECM glycoproteins, exactly in line with our results. As the most prominent node protein in the downregulated PPI network, FN1 emerges as a potential candidate for the restoration of ECM-related functions in monocytes within the tumor microenvironment. However, given the tumorigenic role of elevated FN1 in tumor tissues, substantial and rigorous research efforts are required to validate it.

THBS1 is a stromal cell protein with elevated expression levels observed in the context of inflammation. It serves multiple functions, including the suppression of angiogenesis and modulation of immune responses.[49] Daubon et al. found a specific inhibition of the THBS1/CD47 interaction decreases glioblastoma cell invasion.[50] On the contrary, a recent study suggested that high THBS1 expression is linked to mesenchymal characteristics, immunosuppression, and unfavorable prognosis in CRC.[51] Specifically in macrophages, it is well-documented that THBS1 can activate the inflammatory phenotype of macrophages via a pathway that depends on TLR4.[52] Considering the downregulation of the TLR pathway result, we speculate that CRC cells may dampen the antimicrobial capabilities of monocytes by reducing THBS1 expression. This putative mechanism could potentially synergize with the tumor-promoting activities of intratumoral microbiota. Nonetheless, further in-depth research is required to substantiate this hypothesis.

JUN encodes a protein similar to a viral protein that interacts directly with specific target DNA sequences to regulate gene expression. JUN inhibition affects multiple molecular pathways.[53] As a part of the AP-1 transcription factor complex, JUN is important for monocytic differentiation.[54] Drawing from our simultaneous observations, wherein numerous hub proteins upregulated on monocytes under the influence of CRC cells are highly expressed in M2-type macrophages, we postulate that the downregulation of JUN may represent one of the mechanisms employed by tumors to promote monocyte differentiation toward the M2 phenotype or suppress differentiation toward the M1 phenotype.

To further advance our investigation, we subjected the upregulated DEPs to analysis across multiple clinical databases. Encouragingly, our results have unveiled several promising leads with potential clinical relevance.

By reusing the transcriptome data from peripheral blood monocytes of colorectal cancer patients (GSE47756), TP53I3 has surfaced as a potential diagnostic biomarker with clinical utility. It is the tumor protein p53 inducible protein 3, also called p53-inducible gene 3 (PIG3). Studies often investigate its role in cancer research. Physiologically, P53 controls intracellular reactive oxygen species (ROS) levels coupled with p53R2 to support antioxidant activity by maintaining high catalase levels, protecting against ROS. Under genotoxic stress, elevated p53 and TP53I3 collaborate to inhibit catalase, shifting the balance toward oxidative stress and potentially promoting apoptotic cell death.[55] However, Lee et al.[56] assumed that TP53I3 was a vital component of the DNA damage response pathway, directly facilitating the transmission of DNA damage signals to the intra-S and G2/M checkpoint machinery in human cells. The in vitro experiments[57] showed its ability to colony formation, migration, and invasion in HCT116, the CRC cell line. Whether a similar effect exists in monocytes has yet to be investigated. Hence, the detailed function and the elevated mechanism in the monocytes under tumor secretion stimulation are unclear. Further research is essential to elucidate the functions and mechanisms associated with the elevated expression of TP53I3 in monocytes of cancer patients, as well as to assess its potential clinical diagnostic value. Simultaneously, while CCR1, PLIN2, and S100P may not discriminate between patients with primary and metastatic tumors in the public data, they do exhibit a correlation with disease severity, with their expression levels rising as the disease progresses. Since our results are derived from the protein level while theirs are based on RNA microarray data, the diagnostic potential of these proteins in clinical settings cannot be overlooked. Certainly, further population testing is necessary for validation.

Furthermore, we sought to explore whether there is specific protein expression on monocytes and whether these proteins are correlated with clinical prognosis. To achieve this, we conducted a combined analysis using both scRNA data and the TCGA database and were delighted to uncover four potential indicators with predictive capabilities for clinical prognosis.

ADAMTSL4 is part of the ADAMTS (a disintegrin and metalloproteinase with thrombospondin motifs)-like gene family and is characterized by seven thrombospondin type 1 repeats.[58] It plays a structural role in the body ECM. Glioblastoma is notably enriched[59] and related to poor prognosis.[60] PRAM1 (PML-RARA-regulated adapter molecule 1) is a membrane protein specifically expressed in monocytes. A persistent increase has been identified in the HL-60 cell line (acute myeloid leukemia) under all-trans-retinoid acid treatment, indicating participation in granulocytic differentiation.[61] In the realm of tumor prognosis, limited research has been conducted on these two proteins. Through our cocultivation experiments in conjunction with public databases, we initially observed their distinctive overexpression on monocytes/macrophages within colorectal cancer patient tissues. Furthermore, by harnessing TCGA database analysis, we discerned

https://doi.org/10.1021/acs.jproteome.4c00400
J. Proteome Res. XXXX, XXX, XXX−XXX

a correlation between their elevated expression and unfavorable prognostic outcomes, both in terms of OS and DFS. Moreover, two more proteins were identified as high-risk factors for recurrence. Glycoprotein nonmetastatic melanoma b (GPNMB) is a transmembrane glycoprotein that exhibits elevated expression in various cancer types and a variety of cell types.[62] However, in our analysis of scRNA and bulk data, only monocytes and macrophages highly expressed it and contributed to the short DFS. Robichaud et al.[63] unveiled that soluble GPNMB was mainly produced by M2-polarized macrophages, and its expression in TAMs was associated with aggressive tumor behavior, partly akin to our results. Additionally, NPC2 is one of the essential proteins for lysosomal cholesterol egress.[64] This protein is often explored in cholesterol metabolism, but rarely in cancer. Although NPC2 lacks the same degree of specificity as the aforementioned three proteins, it demonstrates the highest expression on monocytes/macrophages within colorectal tumor tissues. Thus, we also assume that the short recurrence time observed in cases with elevated NPC2 expression is primarily attributed to this subset. Remarkably, the concomitant coexpression of GPNMB and PRAM1 demonstrated a robust correlation with T-cell exhaustion and Treg signatures, even more significant than a recent discovery of MS4A4A.[14] This observation strongly suggests that the presence of GPNMB$^+$PRAM1$^+$TAMs may potentially serve as an indicator of an immunosuppressive TME or function as a suppressor to T cells. However, all the inferences require further experimental validation.

In summary, in vitro coculture of the monocyte cell line THP-1 with six different CRC cell lines was conducted to assess proteomic changes of the monocytes when exposed to cancer cells. Utilizing various analytical approaches, we identified the downregulation of monocyte ECM-related functions and intrinsic immune-related pathways such as the NLR and TLR pathways. This suppression possibly led to the differentiation of monocytes into M2 macrophages and a decline in antimicrobial function, ultimately promoting tumor progression. FN1, THBS1, and JUN were identified as potential key proteins regulated in this context. Furthermore, for the upregulated markers, validation across multiple public databases revealed the potential of monocyte TP53I3 as a diagnostic biomarker for CRC. Notably, the specific high expression of ADAMTSL4, PRAM1, GPNMB, and NPC2 on monocyte/macrophages within tumor tissues was associated with adverse clinical outcomes. Moreover, the GPNMB$^+$PRAM1$^+$TAMs potentially suggest an immunosuppressed condition, which warrants further experimental validation.

Although our findings are based on post-coculture sequencing, our conclusions of pathway analyses have not been experimentally validated, suggesting further functional experiments are necessary to confirm these results. We plan to incorporate experimental validation of our proteomic findings in subsequent studies to confirm these results and further elucidate the mechanisms involved. Our results demonstrated the proteomic landscape of monocytes in response to colorectal cancer cells, providing promising clues for future investigations of the crosstalk between cancer cells and monocytes within the tumor microenvironment.

■ ASSOCIATED CONTENT

Data Availability Statement

Data are available from the corresponding author on a reasonable request.

Supporting Information

The Supporting Information is available free of charge at https://pubs.acs.org/doi/10.1021/acs.jproteome.4c00400.

Assessment of identification and quantitative results. (A) Molecular weight distribution. (B) Isoelectric point distribution. (C) Peptide length distribution. (D) Protein sequence coverage distribution. (E) Peptide count distribution (Figure S1); the similarities and differences in metastatic DEPs and the pathways involved in these DEPs compared with those of all tumor cells versus controls. (A) Venn diagram of DEPs in different groups and the detailed intersection results. (B) Venn diagram of differential KEGG pathways in different groups and the detailed intersection results. CRC_up/down, the DEPs/pathways between all CRC groups and controls; ME_up/down, the DEPs/pathways between metastatic groups and nonmetastatic groups (Figure S2); validation of selected protein-corresponding genes using TCGA data sets. (A−R) The expression levels of 17 upregulated differential proteins corresponding genes during the monocyte-to-macrophage differentiation process. GEPIA2021 was applied for this analysis (Figure S3); validation of selected protein-corresponding genes in the other single-cell transcriptome data set. (A) the single-cell clustering results of the GSE146771 data set. (B) The visualization of 4 selected genes in the GSE146771 data set. (C) Violin plot of selected gene expression levels (Figure S4) (PDF)

Detailed information of identified peptides (Table S1) (XLSX)

Detailed information of identified proteins (Table S2) (XLSX)

Detailed results of differential expressed proteins (Table S3) (XLSX)

Detailed enrichment results of differential expressed proteins (Table S4) (XLSX)

Detailed results of gene set enrichment analysis (Table S5) (XLSX)

Detailed results of weighted correlation network analysis (Table S6) (XLSX)

Detailed results of metastatic part (Table S7) (XLSX)

■ AUTHOR INFORMATION

Corresponding Author

Jie Ma − *Peking University Fifth School of Clinical Medicine, Beijing 100730, China; Center of Biotherapy, Beijing Hospital, National Center of Gerontology, Institute of Geriatric Medicine, Chinese Academy of Medical Sciences, Beijing 100730, China;* orcid.org/0000-0002-2938-818X; Phone: 86-10-85133662; Email: majie4685@bjhmoh.cn

Authors

Yiran Wang − *Peking University Fifth School of Clinical Medicine, Beijing 100730, China; Center of Biotherapy, Beijing Hospital, National Center of Gerontology, Institute of*

https://doi.org/10.1021/acs.jproteome.4c00400
J. Proteome Res. XXXX, XXX, XXX−XXX

Geriatric Medicine, Chinese Academy of Medical Sciences, Beijing 100730, China

Luyao Zhang − *Center of Biotherapy, Beijing Hospital, National Center of Gerontology, Institute of Geriatric Medicine, Chinese Academy of Medical Sciences, Beijing 100730, China*

Jing Xu − *Center of Biotherapy, Beijing Hospital, National Center of Gerontology, Institute of Geriatric Medicine, Chinese Academy of Medical Sciences, Beijing 100730, China*

Complete contact information is available at: https://pubs.acs.org/10.1021/acs.jproteome.4c00400

Author Contributions

Y.W.: writing—original draft, methodology, investigation, data curation, visualization. L.Z.: methodology, validation, writing—reviewing and editing. J.X.: investigation, data curation, validation. J.M.: conceptualization, supervision, project administration, writing—reviewing and editing.

Funding

This study was supported by the National High Level Hospital Clinical Research Funding, grant no. BJ-2022−118 (J.M.) and the National Natural Science Foundation of China, grant no. 82203534 (L.Z.).

Notes

The authors declare no competing financial interest.

■ ACKNOWLEDGMENTS

We wish to express our sincere gratitude to Prof. Simei Ren from The Key Laboratory of Geriatrics, Beijing Institute of Geriatrics, Institute of Geriatric Medicine, Chinese Academy of Medical Sciences, Beijing Hospital/National Center of Gerontology of National Health Commission, P.R. China, for the guidance in cell culture.

■ REFERENCES

(1) Siegel, R. L.; Wagle, N. S.; Cercek, A.; Smith, R. A.; Jemal, A. Colorectal cancer statistics, 2023. *Ca-Cancer J. Clin.* **2023**, *73*, 233−254.

(2) González, N. S.; Salvà, F.; Ros, J.; Baraibar, I.; Rodríguez-Castells, M.; García, A.; et al. Unravelling the Complexity of Colorectal Cancer: Heterogeneity, Clonal Evolution, and Clinical Implications. *Cancers* **2023**, *15*, No. 4020, DOI: 10.3390/cancers15164020.

(3) Baghban, R.; Roshangar, L.; Jahanban-Esfahlan, R.; Seidi, K.; Ebrahimi-Kalan, A.; Jaymand, M.; et al. Tumor microenvironment complexity and therapeutic implications at a glance. *Cell Commun. Signaling* **2020**, *18*, No. 59.

(4) Zhang, H.; Liu, L.; Liu, J.; Dang, P.; Hu, S.; Yuan, W.; et al. Roles of tumor-associated macrophages in anti-PD-1/PD-L1 immunotherapy for solid cancers. *Mol. Cancer* **2023**, *22*, No. 58.

(5) Pathria, P.; Louis, T. L.; Varner, J. A. Targeting Tumor-Associated Macrophages in Cancer. *Trends Immunol.* **2019**, *40*, 310−327.

(6) Auffray, C.; Sieweke, M. H.; Geissmann, F. Blood monocytes: development, heterogeneity, and relationship with dendritic cells. *Annu. Rev. Immunol.* **2009**, *27*, 669−692.

(7) Franklin, R. A.; Liao, W.; Sarkar, A.; Kim, M. V.; Bivona, M. R.; Liu, K.; et al. The cellular and molecular origin of tumor-associated macrophages. *Science* **2014**, *344*, 921−925.

(8) Mantovani, A.; Marchesi, F.; Malesci, A.; Laghi, L.; Allavena, P. Tumour-associated macrophages as treatment targets in oncology. *Nat. Rev. Clin. Oncol.* **2017**, *14*, 399−416.

(9) Mantovani, A.; Allavena, P.; Marchesi, F.; Garlanda, C. Macrophages as tools and targets in cancer therapy. *Nat. Rev. Drug Discovery* **2022**, *21*, 799−820.

(10) Zhang, L.; Wang, Y.; Yuan, W.; An, C.; Tan, Q.; Ma, J. BEST1 Positive Monocytes in Circulation: Visualize Intratumoral Crosstalk between Cancer Cells and Monocytes. *Adv. Sci.* **2023**, *10*, No. e2205915.

(11) Wang, H.; Shao, Q.; Wang, J.; Zhao, L.; Wang, L.; Cheng, Z.; et al. Decreased CXCR2 expression on circulating monocytes of colorectal cancer impairs recruitment and induces Re-education of tumor-associated macrophages. *Cancer lett.* **2022**, *529*, 112−125.

(12) Yin, Y.; Liu, B.; Cao, Y.; Yao, S.; Liu, Y.; Jin, G.; et al. Colorectal Cancer-Derived Small Extracellular Vesicles Promote Tumor Immune Evasion by Upregulating PD-L1 Expression in Tumor-Associated Macrophages. *Adv. Sci.* **2022**, *9*, No. 2102620, DOI: 10.1002/advs.202102620.

(13) Helgason, H.; Eiriksdottir, T.; Ulfarsson, M. O.; Choudhary, A.; Lund, S. H.; Ivarsdottir, E. V.; et al. Evaluation of Large-Scale Proteomics for Prediction of Cardiovascular Events. *JAMA* **2023**, *330*, 725−735.

(14) Li, Y.; Shen, Z.; Chai, Z.; Zhan, Y.; Zhang, Y.; Liu, Z.; et al. Targeting MS4A4A on tumour-associated macrophages restores CD8+ T-cell-mediated antitumour immunity. *Gut* **2023**, *72*, 2307−2320.

(15) Zhang, Y.; Yu, G.; Chu, H.; Wang, X.; Xiong, L.; Cai, G.; et al. Macrophage-Associated PGK1 Phosphorylation Promotes Aerobic Glycolysis and Tumorigenesis. *Mol. Cell* **2018**, *71*, 201−15.e7.

(16) Ashburner, M.; Ball, C. A.; Blake, J. A.; Botstein, D.; Butler, H.; Cherry, J. M.; et al. Gene ontology: tool for the unification of biology. The Gene Ontology Consortium. *Nat. Genet.* **2000**, *25*, 25−29.

(17) Aleksander, S. A.; Balhoff, J.; Carbon, S.; Cherry, J. M.; Drabkin, H. J.; Ebert, D.; et al. The Gene Ontology knowledgebase in 2023. *Genetics* **2023**, *224*, No. iyad031, DOI: 10.1093/genetics/iyad031.

(18) Kanehisa, M.; Goto, S.; Sato, Y.; Furumichi, M.; Tanabe, M. KEGG for integration and interpretation of large-scale molecular data sets. *Nucleic Acids Res.* **2012**, *40*, D109−D114.

(19) Yu, G.; Wang, L. G.; Han, Y.; He, Q. Y. clusterProfiler: an R package for comparing biological themes among gene clusters. *OMICS-J. Integrative Biol.* **2012**, *16*, 284−287.

(20) Luo, W.; Brouwer, C. Pathview: an R/Bioconductor package for pathway-based data integration and visualization. *Bioinformatics* **2013**, *29*, 1830−1831.

(21) Subramanian, A.; Tamayo, P.; Mootha, V. K.; Mukherjee, S.; Ebert, B. L.; Gillette, M. A.; et al. Gene set enrichment analysis: a knowledge-based approach for interpreting genome-wide expression profiles. *Proc. Natl. Acad. Sci. U.S.A.* **2005**, *102*, 15545−15550.

(22) Kerseviciute, I.; Gordevicius, J. aPEAR: an R package for autonomous visualization of pathway enrichment networks. *Bioinformatics* **2023**, *39*, No. btad672, DOI: 10.1093/bioinformatics/btad672.

(23) Langfelder, P.; Horvath, S. WGCNA: an R package for weighted correlation network analysis. *BMC Bioinf.* **2008**, *9*, No. 559.

(24) Bu, D.; Luo, H.; Huo, P.; Wang, Z.; Zhang, S.; He, Z.; et al. KOBAS-i: intelligent prioritization and exploratory visualization of biological functions for gene enrichment analysis. *Nucleic Acids Res.* **2021**, *49*, W317−W325.

(25) Szklarczyk, D.; Gable, A. L.; Nastou, K. C.; Lyon, D.; Kirsch, R.; Pyysalo, S.; et al. The STRING database in 2021: customizable protein-protein networks, and functional characterization of user-uploaded gene/measurement sets. *Nucleic Acids Res.* **2021**, *49*, D605−D612.

(26) Xiao, S.; Zhou, Y.; Wu, Q.; Liu, Q.; Chen, M.; Zhang, T.; et al. FCER1G and PTGS2 Serve as Potential Diagnostic Biomarkers of Acute Myocardial Infarction Based on Integrated Bioinformatics Analyses. *DNA Cell Biol.* **2021**, *40*, 1064−1075.

(27) Otasek, D.; Morris, J. H.; Bouças, J.; Pico, A. R.; Demchak, B. Cytoscape Automation: empowering workflow-based network analysis. *Genome Biol.* **2019**, *20*, No. 185.

(28) Huerta-Cepas, J.; Szklarczyk, D.; Heller, D.; Hernández-Plaza, A.; Forslund, S. K.; Cook, H.; et al. eggNOG 5.0: a hierarchical, functionally and phylogenetically annotated orthology resource based on 5090 organisms and 2502 viruses. *Nucleic Acids Res.* **2019**, *47*, D309−D314.
(29) Li, C.; Tang, Z.; Zhang, W.; Ye, Z.; Liu, F. GEPIA2021: integrating multiple deconvolution-based analysis into GEPIA. *Nucleic Acids Res.* **2021**, *49*, W242−W246.
(30) Hamm, A.; Prenen, H.; Van Delm, W.; Di Matteo, M.; Wenes, M.; Delamarre, E.; et al. Tumour-educated circulating monocytes are powerful candidate biomarkers for diagnosis and disease follow-up of colorectal cancer. *Gut* **2016**, *65*, 990−1000.
(31) Goksuluk, D.; Korkmaz, S.; Zararsiz, G.; Karaagaoglu, A. easyROC: An Interactive Web-tool for ROC Curve Analysis Using R Language Environment. *R J.* **2016**, *8*, 213−230.
(32) Han, Y.; Wang, Y.; Dong, X.; Sun, D.; Liu, Z.; Yue, J.; et al. TISCH2: expanded datasets and new tools for single-cell transcriptome analyses of the tumor microenvironment. *Nucleic Acids Res.* **2023**, *51*, D1425−D1431.
(33) Tang, Z.; Kang, B.; Li, C.; Chen, T.; Zhang, Z. GEPIA2: an enhanced web server for large-scale expression profiling and interactive analysis. *Nucleic Acids Res.* **2019**, *47*, W556−W560.
(34) Bonaventura, P.; Shekarian, T.; Alcazer, V.; Valladeau-Guilemond, J.; Valsesia-Wittmann, S.; Amigorena, S.; et al. Cold Tumors: A Therapeutic Challenge for Immunotherapy. *Front. Immunol.* **2019**, *10*, No. 168.
(35) Xiang, X.; Wang, J.; Lu, D.; Xu, X. Targeting tumor-associated macrophages to synergize tumor immunotherapy. *Signal Transduction Targeted Ther.* **2021**, *6*, No. 75.
(36) Cendrowicz, E.; Sas, Z.; Bremer, E.; Rygiel, T. P. The Role of Macrophages in Cancer Development and Therapy. *Cancers* **2021**, *13*, No. 1946, DOI: 10.3390/cancers13081946.
(37) Shibutani, M.; Maeda, K.; Nagahara, H.; Fukuoka, T.; Nakao, S.; Matsutani, S.; et al. The peripheral monocyte count is associated with the density of tumor-associated macrophages in the tumor microenvironment of colorectal cancer: a retrospective study. *BMC cancer* **2017**, *17*, No. 404.
(38) Karamanos, N. K.; Theocharis, A. D.; Piperigkou, Z.; Manou, D.; Passi, A.; Skandalis, S. S.; et al. A guide to the composition and functions of the extracellular matrix. *FEBS J.* **2021**, *288*, 6850−6912.
(39) Nersisyan, S.; Novosad, V.; Engibaryan, N.; Ushkaryov, Y.; Nikulin, S.; Tonevitsky, A. ECM-Receptor Regulatory Network and Its Prognostic Role in Colorectal Cancer. *Front. Genet.* **2021**, *12*, No. 782699.
(40) de Fougerolles, A. R.; Koteliansky, V. E. Regulation of monocyte gene expression by the extracellular matrix and its functional implications. *Immunol. Rev.* **2002**, *186*, 208−220.
(41) Medrano-Bosch, M.; Simón-Codina, B.; Jiménez, W.; Edelman, E. R.; Melgar-Lesmes, P. Monocyte-endothelial cell interactions in vascular and tissue remodeling. *Front. Immunol.* **2023**, *14*, No. 1196033.
(42) Li, D.; Wu, M. Pattern recognition receptors in health and diseases. *Signal Transduction Targeted Ther.* **2021**, *6*, No. 291.
(43) Coillard, A.; Guyonnet, L.; De Juan, A.; Cros, A.; Segura, E. TLR or NOD receptor signaling skews monocyte fate decision via distinct mechanisms driven by mTOR and miR-155. *Proc. Natl. Acad. Sci. U.S.A.* **2021**, *118*, No. e2109225118, DOI: 10.1073/pnas.2109225118.
(44) Liu, J.; Zhang, Y. Intratumor microbiome in cancer progression: current developments, challenges and future trends. *Biomarker Res.* **2022**, *10*, No. 37.
(45) VanSlyke, J. K.; Boswell, B. A.; Musil, L. S. Fibronectin regulates growth factor signaling and cell differentiation in primary lens cells. *J. Cell Sci.* **2018**, *131*, No. jcs217240, DOI: 10.1242/jcs.217240.
(46) Sahai, E.; Astsaturov, I.; Cukierman, E.; DeNardo, D. G.; Egeblad, M.; Evans, R. M.; et al. A framework for advancing our understanding of cancer-associated fibroblasts. *Nat. Rev. Cancer* **2020**, *20*, 174−186.
(47) Yang, D.; Liu, J.; Qian, H.; Zhuang, Q. Cancer-associated fibroblasts: from basic science to anticancer therapy. *Exp. Mol. Med.* **2023**, *55*, 1322−1332.
(48) Madsen, D. H.; Jürgensen, H. J.; Siersbæk, M. S.; Kuczek, D. E.; Grey Cloud, L.; Liu, S.; et al. Tumor-Associated Macrophages Derived from Circulating Inflammatory Monocytes Degrade Collagen through Cellular Uptake. *Cell Rep.* **2017**, *21*, 3662−3671.
(49) Kaur, S.; Bronson, S. M.; Pal-Nath, D.; Miller, T. W.; Soto-Pantoja, D. R.; Roberts, D. D. Functions of Thrombospondin-1 in the Tumor Microenvironment. *Int. J. Mol. Sci.* **2021**, *22*, No. 4570, DOI: 10.3390/ijms22094570.
(50) Daubon, T.; Léon, C.; Clarke, K.; Andrique, L.; Salabert, L.; Darbo, E.; et al. Deciphering the complex role of thrombospondin-1 in glioblastoma development. *Nat. Commun.* **2019**, *10*, No. 1146.
(51) Omatsu, M.; Nakanishi, Y.; Iwane, K.; Aoyama, N.; Duran, A.; Muta, Y.; et al. THBS1-producing tumor-infiltrating monocyte-like cells contribute to immunosuppression and metastasis in colorectal cancer. *Nat. Commun.* **2023**, *14*, No. 5534.
(52) Li, Y.; Qi, X.; Tong, X.; Wang, S. Thrombospondin 1 activates the macrophage Toll-like receptor 4 pathway. *Cell. Mol. Immunol.* **2013**, *10*, 506−512.
(53) Zhou, C.; Martinez, E.; Di Marcantonio, D.; Solanki-Patel, N.; Aghayev, T.; Peri, S.; et al. JUN is a key transcriptional regulator of the unfolded protein response in acute myeloid leukemia. *Leukemia* **2017**, *31*, 1196−1205.
(54) Zhao, X.; Bartholdy, B.; Yamamoto, Y.; Evans, E. K.; Alberich-Jordà, M.; Staber, P. B.; et al. PU.1-c-Jun interaction is crucial for PU.1 function in myeloid development. *Commun. Biol.* **2022**, *5*, No. 961.
(55) Kang, M. Y.; Kim, H. B.; Piao, C.; Lee, K. H.; Hyun, J. W.; Chang, I. Y.; You, H. J. The critical role of catalase in prooxidant and antioxidant function of p53. *Cell Death Differ.* **2013**, *20*, 117−129.
(56) Lee, J. H.; Kang, Y.; Khare, V.; Jin, Z. Y.; Kang, M. Y.; Yoon, Y.; et al. The p53-inducible gene 3 (PIG3) contributes to early cellular response to DNA damage. *Oncogene* **2010**, *29*, 1431−1450.
(57) Park, S. J.; Kim, H. B.; Kim, J.; Park, S.; Kim, S. W.; Lee, J. H. The oncogenic effects of p53-inducible gene 3 (PIG3) in colon cancer cells. *Korean J. Physiol. Pharmacol.* **2017**, *21*, 267−273.
(58) Mead, T. J.; Apte, S. S. ADAMTS proteins in human disorders. *Matrix Biol.* **2018**, *71*−*72*, 225−239.
(59) Zhao, Z.; Zhang, K. N.; Chai, R. C.; Wang, K. Y.; Huang, R. Y.; Li, G. Z.; et al. ADAMTSL4, a Secreted Glycoprotein, Is a Novel Immune-Related Biomarker for Primary Glioblastoma Multiforme. *Dis. markers* **2019**, *2019*, No. 1802620.
(60) Wu, C.; Qin, C.; Long, W.; Wang, X.; Xiao, K.; Liu, Q. Tumor antigens and immune subtypes of glioblastoma: the fundamentals of mRNA vaccine and individualized immunotherapy development. *J. Big Data* **2022**, *9*, No. 92.
(61) Novikova, S.; Tolstova, T.; Kurbatov, L.; Farafonova, T.; Tikhonova, O.; Soloveva, N.; et al. Nuclear Proteomics of Induced Leukemia Cell Differentiation. *Cells* **2022**, *11*, No. 3221, DOI: 10.3390/cells11203221.
(62) Lazaratos, A. M.; Annis, M. G.; Siegel, P. M. GPNMB: a potent inducer of immunosuppression in cancer. *Oncogene* **2022**, *41*, 4573−4590.
(63) Robichaud, S.; Fairman, G.; Vijithakumar, V.; Mak, E.; Cook, D. P.; Pelletier, A. R.; et al. Identification of novel lipid droplet factors that regulate lipophagy and cholesterol efflux in macrophage foam cells. *Autophagy* **2021**, *17*, 3671−3689.
(64) Qian, H.; Wu, X.; Du, X.; Yao, X.; Zhao, X.; Lee, J.; et al. Structural Basis of Low-pH-Dependent Lysosomal Cholesterol Egress by NPC1 and NPC2. *Cell* **2020**, *182*, 98−111.e18.

https://doi.org/10.1021/acs.jproteome.4c00400
J. Proteome Res. XXXX, XXX, XXX−XXX